

Calculated phonon band structure and density of states and interpretation of the Raman spectrum in rocksalt ScN

Tula R. Paudel and Walter R. L. Lambrecht

Department of Physics, Case Western Reserve University, Cleveland, Ohio 44106-7079, USA

(Received 23 July 2008; revised manuscript received 16 October 2008; published 13 February 2009)

The first-principles linear-response method is used to calculate the phonons in rocksalt ScN in the local-density approximation. The calculated density of phonon states is compared with Raman spectra in the literature, which are interpreted as disorder-induced first-order Raman spectra and provide information mostly on zone-boundary Raman modes.

DOI: [10.1103/PhysRevB.79.085205](https://doi.org/10.1103/PhysRevB.79.085205)

PACS number(s): 78.30.-j, 63.20.dk

I. INTRODUCTION

As one of the simplest transition-metal nitrides, ScN is quite interesting. After this material was thought to be a semimetal for a long time,¹ it was finally concluded to be a semiconductor with an indirect gap of about 1 eV and smallest direct gap of about 2 eV.²⁻⁷ It was recently found to be a potentially interesting magnetic semiconductor host by adding Mn as dopant.^{8,9} Its crystal growth in thin-film form was improved considerably in recent years.^{4,10-12} It was also predicted that alloys or superlattices with IIIa column elements Ga, Al, or In might have interesting properties involving a hexagonal form of ScN.¹³⁻¹⁵ Yet, several properties of this material are only poorly known. Here we study the vibrational properties. While calculated phonon band structures were reported previously for the hypothetical hexagonal form,¹⁴ we are only aware of one previous study of the phonons in rocksalt ScN.¹⁶ That paper does not discuss the comparison with the Raman spectra in any detail and furthermore uses a different pseudopotential from the one used here, which leads to significant differences.

In the rocksalt structure, first-order Raman scattering is forbidden by symmetry. Yet, a Raman spectrum was observed and reported by Travaglini *et al.*¹ and by Gu *et al.*¹² It was interpreted as a disorder-induced first-order Raman spectrum representing the density of phonon states. In infrared absorption, one expects to see the TO and LO modes at the zone center because these are optically allowed, but the presence of free carriers complicates this picture. Travaglini *et al.*¹ extracted ω_{TO} to be 45 meV or 362 cm^{-1} from an analysis of the infrared reflectivity, which exhibits a plasmon LO-phonon-coupled mode because of the large free-carrier concentration in their samples.

Here, we present phonon band structures and density of states (DOS) and compare carefully with the Raman data by Travaglini *et al.*¹ We find that the latter shows not a pure but weighted density of states, with a larger intensity for the LO(L) modes. Several features can be accounted for with Van Hove singularities at the zone boundary. The emphasis of the LO(L) modes is explained in terms of their dominant role in the breathing-induced motions around the cation which exhibit the strongest electron-phonon coupling.

II. METHODS

The calculations of the phonons are performed using the linear-response approach in the local-density approximation

(LDA) combined with a pseudopotential plane-wave basis set band-structure method as implemented in the open source ABINIT code.¹⁷⁻¹⁹ A small core pseudopotential in which the 3s and 3p electrons are not pseudized but treated as valence electrons is used.²⁰ The same hard pseudopotentials were also used by Ranjan *et al.*¹⁴ in their study of hexagonal ScN and they found the structural properties obtained with it to be in good agreement with those obtained from ultrasoft pseudopotentials. The Brillouin-zone integrations are carried out with a $6 \times 6 \times 6$ mesh and a plane-wave cutoff of 80 Ry is used. We use the experimental lattice constant of 4.50 Å which is close to our calculated equilibrium lattice constant of 4.48 Å.

III. RESULTS

Our results for some of the phonons at symmetry points are given in Table I. Our value of 365 cm^{-1} for $\omega_{\text{TO}}(\Gamma)$ is in excellent agreement with the value of 362 cm^{-1} extracted from the infrared reflectivity by Travaglini *et al.*¹ taking into account the coupling to free carriers. In contrast, Duman *et al.*¹⁶ obtained a significantly lower value 270 cm^{-1} for the TO(Γ) mode and 601 cm^{-1} for the LO(Γ) mode as a result

TABLE I. Phonon frequencies in cm^{-1} for ScN.

Mode	$\omega_j(\mathbf{q})$
TO(Γ)	365
LO(Γ)	632
TA(L)	234
LA(L)	464
TO(L)	460
LO(L)	657
TA(X)	267
LA(X)	354
TO(X)	415
LO(X)	569
TA(W)	321
LA(W)	329
TO(W)	518
LO(W)	543

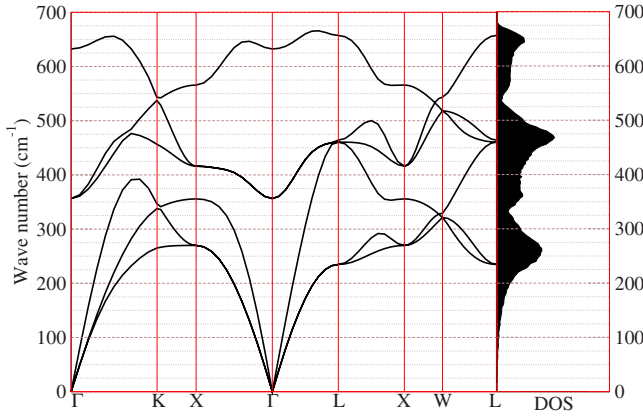


FIG. 1. (Color online) Phonon band structure and density of states in ScN.

of their use of a different pseudopotential treating $3s$ and $3p$ electrons as core rather than band. They state in their paper that these are in reasonable agreement with experimental Raman data but were compared to Travaglini's result which is obtained from the infrared rather than the Raman data. As clearly stated by Travaglini *et al.*¹ the Raman data they measured corresponds to a weighted density of states instead of phonons at the Γ point. We discuss this more fully below. Meanwhile, our value for the LO mode at Γ is substantially lower than the value of 155 meV or 1250 cm^{-1} obtained by Travaglini *et al.*¹ as the zero in the phonon part of the dielectric constant extracted from their actual data by a model for the coupling to free carriers and also including interband transitions. The latter was in part based on a LDA band structure which underestimates the gap significantly and led them to the assumption that ScN is a semimetal. It is now known that ScN is in fact a semiconductor. So, in retrospect, we must conclude that the value for the LO mode given by Travaglini *et al.*¹ is not very reliable. It seems excessively high compared to the LO(L) phonon mode.

The phonon dispersion along lines connecting high-symmetry points of the Brillouin zone and the corresponding DOS are shown in Fig. 1.

The Raman spectrum of ScN was interpreted by Travaglini *et al.*¹ as a disordered-induced first-order Raman spectrum. The origin of the disorder is not entirely clear. It may at least in part arise from the presence of nitrogen vacancies. They labeled peaks at 44 , 51.9 , and 84 meV corresponding to 355 , 419 , and 677 cm^{-1} respectively. However, one can actually discern more detailed structure in their spectra, which for convenience is here reproduced in Fig. 2 and juxtaposed with our calculated DOS. A summary of the major features comparing theory and experiment is given in Table II.

The first two peaks are quite weak in the experiment and riding on the shoulder of the elastic peak. In the phonon band structure, one can see that the TA bands are flat near L and X , which are M_1 - and M_2 -type saddle-point Van Hove singularities, straddling the peak in the DOS. The next peak is significantly stronger and corresponds to the LA branch which is quite flat along X - W and X - K and gives rise to the peak in the DOS starting at about 350 cm^{-1} . This is also just below the minimum of the TO branch at Γ , but the latter is not

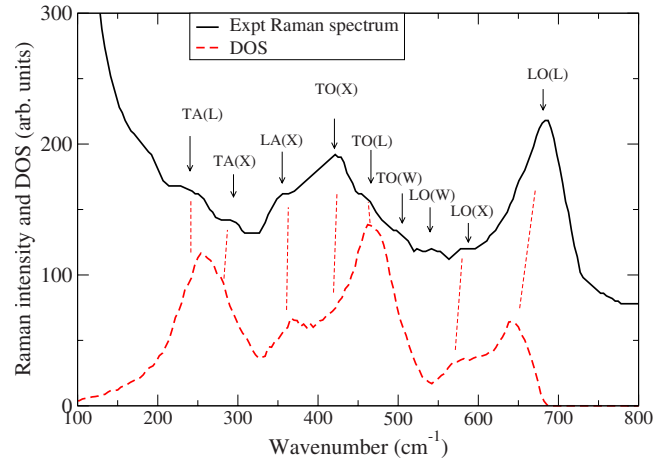


FIG. 2. (Color online) Raman spectrum of ScN by Travaglini *et al.* (Ref. 1) compared to calculated density of states. Peaks corresponding to Van Hove singularities are labeled.

expected to show up particularly strongly if there is no conservation of crystal momentum. The peak at 419 cm^{-1} is the strongest one in the range 300 – 550 cm^{-1} and corresponds well in frequency with the TO(X) although the latter does not show up very strongly in the DOS. The TO(X) is related to an M_1 saddle point with relatively flat dispersion along X - Γ . The main peak in the DOS occurs slightly above the TO(L) frequency, which almost equals the LA(L). This peak is only a relatively weak shoulder in the experiment at about 468 cm^{-1} . Two more weak peaks show in this region before we reach a minimum. We tentatively assign them to the TO(W) and LO(W) modes at W . After the minimum, the Raman spectrum shows an onset at 589 cm^{-1} followed by the strongest experimental Raman peak with a maximum at 677 cm^{-1} . The latter clearly corresponds to the LO(L) M_2 -type singularity. We tentatively assign the 589 cm^{-1} onset to LO(X). We note that the LO-TO splitting is somewhat underestimated by the calculation, which may in part be because of the LDA, which underestimates band gaps; hence overestimates screening and hence underestimates Born effective charges, proportional to the LO-TO splitting. Our cal-

TABLE II. Comparison of experimental Raman spectral peak positions of ScN with calculated phonon frequencies (in cm^{-1}).

Expt.	Calc.	Assignment
242	234	TA(L)
298	267	TA(X)
355	354	LA(X)
	365	TO(Γ)
419	415	TO(X)
468	460	TO(L)
	464	LA(L)
508	516	TO(W)
540	545	LO(W)
589	569	LO(X)
677	657	LO(L)

culated Born effective charge is 4.04. We also obtain the high-frequency and static dielectric constants from the ABINIT calculations to be 12.16 and 38.25. This closely obeys the Lyddane-Sachs-Teller relation,

$$\left[\frac{\omega_{\text{LO}}(\Gamma)}{\omega_{\text{TO}}(\Gamma)} \right]^2 = \frac{\epsilon_0}{\epsilon_\infty}, \quad (1)$$

which is no surprise as this is built into the calculations. Reliable experimental values on the dielectric constant are difficult to obtain in view of the high carrier concentration usually found in ScN.¹ The previous computational study by Duman *et al.*¹⁶ used the generalized gradient approximation (GGA) instead of LDA. As is well known, GGA tends to overestimate lattice constants slightly while LDA tends to underestimate them and, correspondingly, one may expect a trend of slightly overestimating optical modes in LDA and underestimating them in GGA. The difference amounts usually to a few percent and thus using GGA would not qualitatively change any of our conclusions. In fact, here we used the experimental lattice constant and obtained excellent agreement for the TO mode at Γ . The more important computational difference with Duman *et al.*'s work¹⁶ is their use of a softer and less accurate pseudopotential.

Although the Raman spectrum clearly shows features corresponding to $\mathbf{q} \neq 0$, it is not quite proportional to the DOS. It is remarkable that in the experimental Raman spectrum, the main LO peak is stronger than the main TO peak, whereas the opposite is true in the DOS. Also, the DOS appears to peak near the frequency of the TO(L) mode whereas the TO peak of the Raman spectrum has its maximum near the TO(X) frequency. Gu *et al.*¹² found a similarly shaped Raman spectrum in the TO region with a maximum at 425 cm^{-1} but a much weaker LO peak. The slight shift of the TO peak may be indicative of strain in their thin film compared to the bulk samples of Travaglini *et al.*¹ The relative intensity of LO and TO peaks apparently depends sensitively on crystalline quality. Both used 514 nm excitation, which corresponds to 2.4 eV and in ScN is just above the main direct absorption edge.

It is interesting that the LO(L) lines are also strongly weighted in the spin-disorder-induced Raman spectra of EuS.^{21,22} In that case, it was pointed out that these modes are the ones that contribute most strongly to the fully symmetric Γ_1 symmetry displacement of ions around the cation, i.e., to a breathing mode around the cation. These have the strongest electron-phonon coupling. In fact, they show that the Raman intensity under these conditions is given by

$$\frac{d^2\sigma}{d\Omega d\omega'} \propto \sum_{j,\mathbf{q}} \{n[\omega_j(\mathbf{q}), T] + 1\} \delta[\omega - \omega' - \omega_j(\mathbf{q})] \times \left| \sum_{\alpha=1}^3 \frac{e_\alpha(j, \mathbf{q}) \sin(q_\alpha r_0)}{[\omega_j(\mathbf{q})]^{1/2}} \right|^2, \quad (2)$$

where $\omega_j(\mathbf{q})$ is the frequencies of mode j at wave vector \mathbf{q} , $n[\omega_j(\mathbf{q}), T]$ is the boson occupation factor at temperature T , $e_\alpha(j, \mathbf{q})$ is the normalized anion displacement in direction α for this mode, and r_0 is the nearest-neighbor distance. The last factor was shown by them to be strongly weighted for the LO(L) modes. In fact, it maximizes at L and is zero for Γ . This strong breathing mode electron-phonon coupling in the Eu chalcogenide case is related to the fact that the above band gap absorption corresponds to an $f \rightarrow d$ transition, which thus changes the Eu^{2+} to an Eu^{3+} ion, with a corresponding strong change in ionic radius. This may be expected to induce breathing-type vibrations around the cation. In the present case, no f states are present, so this explanation does not carry over directly. However, any transition from valence band to conduction band corresponds to a transition from bonding to more antibonding (Sc $3d$ to N $2p$) combinations of orbitals. This also affects the local bond length and similarly can be expected to couple most strongly to breathing-type vibrations. This may thus also here account for the strong weighting of the LO(L) modes.

IV. CONCLUSIONS

In conclusion, we presented calculated phonon spectra of rocksalt ScN and found them to be in good agreement with Raman spectra and infrared data. The detailed interpretation of the Raman spectrum as a disorder-induced first-order spectrum gives useful information on several zone-boundary modes.

Note added in proof. Recently, we became aware of a related paper²³ which gives similar Raman results for ScN and *ab initio* calculations of phonons along $\Gamma-X$ in fair agreement with ours.

ACKNOWLEDGMENTS

This work was supported by the National Science Foundation Materials Network under Grant No. DMR-0710485. The calculations were performed at the Ohio Supercomputing Center. We thank H. J. Trodahl and R. Merlin for helpful discussions.

¹G. Travaglini, F. Marabelli, R. Monnier, E. Kaldis, and P. Wachter, Phys. Rev. B **34**, 3876 (1986).

²T. D. Moustakas, R. J. Molnar, and J. P. Dismukes, Electrochem. Soc. Proc. **96-11**, 197 (1996).

³W. R. L. Lambrecht, Phys. Rev. B **62**, 13538 (2000).

⁴D. Gall, M. Stadele, K. Jarrendahl, I. Petrov, P. Desjardins, R. T. Haasch, T.-Y. Lee, and J. E. Greene, Phys. Rev. B **63**, 125119

(2001).

⁵C. Stampfl, W. Mannstadt, R. Asahi, and A. J. Freeman, Phys. Rev. B **63**, 155106 (2001).

⁶A. Qteish, P. Rinke, M. Scheffler, and J. Neugebauer, Phys. Rev. B **74**, 245208 (2006).

⁷M. E. Little and M. E. Kordes, Appl. Phys. Lett. **78**, 2891 (2001).

- ⁸A. Herwadkar and W. R. L. Lambrecht, *Phys. Rev. B* **72**, 235207 (2005).
- ⁹A. Herwadkar, W. R. L. Lambrecht, and M. van Schilfgaarde, *Phys. Rev. B* **77**, 134433 (2008).
- ¹⁰H. A. Al-Britthen, A. R. Smith, and D. Gall, *Phys. Rev. B* **70**, 045303 (2004).
- ¹¹A. R. Smith, H. A. H. AL-Britthen, D. C. Ingram, and D. Gall, *J. Appl. Phys.* **90**, 1809 (2001).
- ¹²Z. Gu, J. H. Edgar, J. Pomeroy, M. Kuball, and D. W. Coffeey, *J. Mater. Sci.: Mater. Electron.* **15**, 555 (2004).
- ¹³V. Ranjan, L. Bellaiche, and E. J. Walter, *Phys. Rev. Lett.* **90**, 257602 (2003).
- ¹⁴V. Ranjan, S. Bin-Omran, D. Sichuga, R. S. Nichols, L. Bellaiche, and A. Alsaad, *Phys. Rev. B* **72**, 085315 (2005).
- ¹⁵V. Ranjan, S. Bin-Omran, L. Bellaiche, and A. Alsaad, *Phys. Rev. B* **71**, 195302 (2005).
- ¹⁶S. Duman, S. Bağcı, H. M. Tütüncü, G. Uğur, and G. P. Srivastava, *Diamond Relat. Mater.* **15**, 1175 (2006).
- ¹⁷X. Gonze, *Phys. Rev. B* **55**, 10337 (1997).
- ¹⁸X. Gonze and C. Lee, *Phys. Rev. B* **55**, 10355 (1997).
- ¹⁹X. Gonze, J.-M. Beuken, R. Caracas, F. Detraux, M. Fuchs, G. M. Rignanese, L. Sindic, M. Verstraete, G. Zerah, and F. Jollet, *Comput. Mater. Sci.* **25**, 478 (2002).; <http://www.abinit.org>.
- ²⁰C. Hartwigsen, S. Goedecker, and J. Hutter, *Phys. Rev. B* **58**, 3641 (1998).
- ²¹G. Güntherodt, R. Merlin, and P. Grünberg, *Phys. Rev. B* **20**, 2834 (1979).
- ²²R. Merlin, R. Zeyher, and G. Güntherodt, *Phys. Rev. Lett.* **39**, 1215 (1977).
- ²³D. Gall, M. Stoehr, and J. E. Greene, *Phys. Rev. B* **64**, 174302 (2001).